Title	The effect of carrier-induced change on the optical properties of AlGaAs-GaAs intermixed quantum wells
Author(s)	Chan, CY; Kwok, PCK; Li, EH
Citation	IEEE Journal on Selected Topics in Quantum Electronics, 1998, v. 4 n. 4, p. 685-694
Issued Date	1998
URL	http://hdl.handle.net/10722/42820
Rights	Creative Commons: Attribution 3.0 Hong Kong License

The Effect of Carrier-Induced Change on the Optical Properties of AlGaAs–GaAs Intermixed Quantum Wells

Michael C. Y. Chan, Paul C. K. Kwok, *Member, IEEE*, and E. Herbert Li, *Senior Member, IEEE*

***Abstract*— The carrier-induced effects in the change of absorption and refractive index on the AlGaAs–GaAs intermixing modified quantum wells (QW's) have been investigated theoretically. Band-filling, bandgap shrinkage, and free-carrier absorption have been included for various carrier concentrations. The Schrödinger and the Poisson equations have been considered self-consistently. The polarized absorption coefficients are calculated using the Kane $\mathrm{k}\cdot\mathrm{p}$ method for a four band model and followed by the Kramers–Krönig transformation to obtain the refractive index change. The results obtained show a more enhanced bandgap renormalization and change of absorption, but a reduced change in refractive index for the larger intermixing extents. It is important to know the carrier-induced optical parameter changes the intermixed QW's because of their recent interests in photonics.**

***Index Terms*— Charge carrier processes, optical refraction, quantum-well interdiffusion, quantum-well intermixing, quantum wells.**

I. Introduction

RECENT INTEREST in lasers and modulators has led many researchers to investigate the carrier-induced effects on semiconductors. Theory and experimental results show that the interactions between carriers (electron–electron, hole–hole, and electron–hole) may cause the emission wavelength (energy) to shift, which is known as bandgap renormalization [1]. In addition, they will also result in a change of absorption coefficient and thus a change in refractive index in the semiconductor materials, such as bulk and quantum well (QW) structures including nonsquare shape well produced by alloy composition intermixing in thermally diffused QW (DFQW) [2]. As a consequence, the carrier-induced effect is very important in the design of photonic devices such as switches [3], modulators [4] and filters [5]. Moreover, the carrier-induced refractive index changes are also important for laser design [6] and as new optical probing techniques for GaAs devices as well.

In terms of the effect of the carrier on the optical properties in QW structures, a handful of reports are available. Tourita and Suzuki [7] proposed a self-consistent method in solving eigenvalues and eigen-functions when carriers were injected in a square QW. However, they have not considered the optical parameter changes due to carrier injection, which was very important in the design of optical devices. Some researchers have also reported on the self-consistent calculation of subband structure and optical spectral of a heavily doped n-type GaAs–GaAlAs superlattice [8]. Recently, Chen, Juang, and Chang [9] presented a report on the carrier-induced effects on the energy shift in GaAs–AlGaAs multiple quantum well laser diodes. The authors emphasised the fact that little work had been reported to apply a self-consistent manner to the bandgap shrinkage effect to treat MQW lasers systematically, though there already existed a number of models. However, only optical gain was considered in this paper and only a bulk refractive index was used. In addition, some researchers perform detailed investigation on the injected carrier effects on the carrier-induced shift and broadening of optical spectra in an AlGaAs–GaAs QW with a gate electrode [10], and on the changes in the absorption and refractive index for intersubband optical transitions in GaAs–AlGaAs QW's [11], as well as on the tensile-strained multiple QW structure [12]. Also, the excitonic quenching effects in absorption and refractive index has been reported [13]. In fact, the carrier-induced effects in the change of absorption coefficient and that of refractive index are still not available comprehensively.

In this paper, the main aim is to investigate the effects of carrier-induced changes in absorption coefficient as well as refractive index of the GaAs–$\mathrm{Al}_w\mathrm{Ga}_{1-w}\mathrm{As}$ DFQW. There has been no reports (both experimentally and theoretically) so far on the corresponding research. This study has a considerable significance on the design of devices such as modulation doped photodetectors, QW lasers, photonic switches, and modulators. In Section II, the DFQW confinement profile is obtained with different diffusion lengths. The energy levels and their associated wavefunctions in these DFQW structures are calculated by solving both the Schrödinger and the Poisson equations self-consistently. It is followed by calculating the absorption coefficient for TE and TM polarizations, and followed by the absorption coefficient change, which is defined as the difference between the absorption coefficient with carrier injection in QW and that without carrier injection. The change in refractive index can be determined directly by applying Kramers–Krönig transformation. In Section III, the results obtained from the model and their analysis will be presented. Finally conclusions will be drawn in Section IV.

Manuscript received March 2, 1998; revised June 1, 1998.

The authors are with the Department of Electrical and Electronic Engineering, University of Hong Kong, Pokfulam Road, Hong Kong.

Publisher Item Identifier S 1077-260X(98)06800-2.

II. Model

In this paper, the focus will be on the carrier-induced changes in absorption coefficient and refractive index for GaAs–$Al_wGa_{1-w}As$ DFQW. Three carrier effects are included, namely: bandgap shrinkage, band-filling, free-carrier absorption.

A. Band Structure of DFQW with Carrier Injection

The QW structure to be modeled here is an unstrained AlGaAs–GaAs single QW, which is undoped and free of unintentional impurities. The carriers are assumed to be injected into the QW region from outside at the two end of the thick (>50 nm) barriers. The intermixing process is characterized by a diffusion length L_d defined as $L_d = (Dt)^{1/2}$, where D and t are the diffusion coefficient and annealing time, respectively. The intermixed Al composition profile $w(z)$ across the QW structure is given by:

$$w(z) = w_0\left\{1 - \frac{1}{2}\left[\mathrm{erf}\left(\frac{\frac{1}{4}(L_z+2z)}{L_d}\right) + \mathrm{erf}\left(\frac{\frac{1}{4}(L_z-2z)}{L_d}\right)\right]\right\} \quad (1)$$

where w_0 is the as-grown Al fraction in the barrier, L_z is the as-grown width of the QW, z is both the quantization and the growth axis (QW centered at $z = 0$) and erf denotes the error function. Equation (1) is used to obtain the intermixing induced bandgap $E_g(z) = E_g(w = w(z))$ and other spatially varied intermixing parameters, such as effective mass and dielectric constants. The intermixing induced QW confinement profile is defined here by

$$U_r(z) = Q_r[E_g(z) - E_g(z=0)] \quad (2)$$

where the subscript r denotes the electrons (e) in the conduction band $(r = c)$, and heavy or light holes in the valence band are represented by ($r = v =$ hh or lh). Also the zero potential is defined as that at the bottom of the QW without carriers, and Q_r is the band offset splitting ratio.

In the envelope function scheme with the Ben-Daniel and Duke model [14] using a position dependent effective mass, the DFQW subband edge in the Γ-valley can be calculated by the one-dimensional Schrödinger-like equation. The envelope function $\Psi_{r\ell}(z)$ and eigenenergy $E_{r\ell}$ can be solved by

$$-\frac{\hbar^2}{2}\frac{d}{dz}\left[\frac{1}{m^*_{\perp r}(z)}\frac{d\Psi_{r\ell}(z)}{dz}\right] + U_r(z)\Psi_{r\ell}(z) = E_{r\ell}\Psi_{r\ell}(z) \quad (3)$$

where $\ell = 1, 2, \cdots$ are the QW subband levels for either the electrons, heavy holes, or light holes respectively, $m^*_{\perp r}(w = w(z))$ is the carrier effective mass in the z direction (denoted by $\perp$), $E_{r\ell}$ is the subband-edge energy, and the origin of the potential energy is taken at the bottom of the DFQW. Equation (3) is solved numerically using a finite difference method with the confinement profile defined in (2) and the boundary condition is taken to be zero at the end of the barrier ($\Psi_{r\ell}(z_b) \approx 0, z_b = 50$ nm) [15]. It should be noted that the confinement profiles for electrons, heavy holes and light holes will be further modified according to the carrier injected into the QW.

Here, we consider one of the carrier effects: Bandgap shrinkage. The basic mechanism of bandgap shrinkage is that the injected electrons will occupy states at the bottom of the conduction band. If the concentration of electrons is large enough, the electron wave functions will overlap, forming a gas of interacting particles. The electrons will repel one another by the repulsive Coulombic forces. In addition, electrons having the same spin will try to repel one another which results in screening of electrons and a decrease of their energy, thus, lowering the energy of the conduction band edge arises. A similar corresponding effect for holes increases the energy of the valence band edge. The sum of these effects accounts for bandgap shrinkage. Bandgap shrinkage effects are mainly dependent on free-carrier density, and are nearly independent of impurity concentration.

In this paper, both electrons and holes are treated self-consistently. The initial potential profile $V_{0,r}(z)$ for electrons, heavy and light holes are already given by (3), i.e., $U_r(z) = V_{0,r}(z)$. By solving (3) we can solve for $E_{r\ell}$ and $\Psi_{r\ell}$, which is the energy level and wave function for the ℓth sublevel respectively. The electron, heavy and light hole distributions are denoted by $n_e(z)$, $p_{\mathrm{hh}}(z)$, and $p_{\mathrm{lh}}(z)$, respectively, and are obtained from the solution of the Schrödinger equation as [7]

$$\left.\begin{matrix} n_e(z) \\ p_v(z) \end{matrix}\right\} = \sum_\ell |\Psi_{r\ell}|^2 f_r(E_{r\ell}, E_r) \quad (4)$$

$$N_0 = \frac{1}{L_z}\int_{-z_b}^{+z_b} n_e(z)\,dz \quad (5a)$$

$$P_0 = \frac{1}{L_z}\int_{-z_b}^{+z_b} p_{\mathrm{hh}}(z)\,dz + \frac{1}{L_z}\int_{-z_b}^{+z_b} p_{\mathrm{lh}}(z)\,dz \quad (5b)$$

where f_r is the Fermi–Dirac distribution function and E_r is the Fermi energy, N_0 and P_0 are the carrier density of the hole and electron density, respectively, and L_z is the well width in the z direction.

The Fermi–Dirac distribution functions are given by:

$$f_c(E_t) = \frac{1}{1+\exp[(E_g+E_{c,v}+(m_r/m_e)E_t - E_{fc})/(k_BT)]}$$
$$f_v(E_t) = \frac{1}{1+\exp[(E_{c,v} - (m_r/m_h)E_t - E_{fv})/(k_BT)]} \quad (6)$$

where $E_t = (\hbar^2k^2)/2m_0$, m_r is the reduce mass of electron and holes in the transverse direction.

The quasi-Fermi energy is obtained by the self-consistent calculation. Using the given initially set carrier density (N or P) in (5), a value of quasi-Fermi energy in the Fermi–Dirac distribution is initially guessed and then inserted in (4) to obtain an initial guess of the N_0 and P_0. These carrier distributions is used in (5) to obtain the estimated carrier density. By comparing the estimated carrier density in (5) with the initial set N and P, the value of the quasi-Fermi energy can be obtained if the difference between the initially set N and P and the estimated carrier density [from (5)] is small. This guessing procedure of the quasi-Fermi energy can be looped

iteratively until the values of carrier density converge (within ~1%).

Once the carrier spatial distributions are obtained, we can then estimate the many-body carrier effects, namely the Hartree term and exchange-correlation term. Hartree terms V_{He}, V_{Hhh}, and V_{Hlh} are obtained from the Poisson equation, as

$$\begin{aligned} \frac{d^2}{dz^2}V_{\mathrm{He}}(z) &= -\frac{4\pi e}{\kappa}(p_{\mathrm{hh}}(z)+p_{\mathrm{lh}}(z)-n_e(z)) \\ V_{\mathrm{Hhh}}(z) &= V_{\mathrm{Hlh}}(z) = -V_{\mathrm{He}}(z) \end{aligned} \tag{7}$$

$\kappa = \kappa(w)$ is the dielectric constant. The boundary condition is taken as $V_{\mathrm{Hhh}}(z)$, $V_{\mathrm{Hlh}}(z)$ and $V_{\mathrm{He}}(z)$ equal zero at $z_b = \pm$ 50 nm. The exchange-correlation term V_{xc} is given by

$$\begin{aligned} V_{xc,r}(z) &= -\frac{2}{\pi\beta r_0}[1+0.0545 r_0 \ln(1+11.4/r_0)] \\ \frac{4\pi}{3}r_0^3 &= \frac{1}{n_e} = \frac{1}{p_v} \end{aligned} \tag{8}$$

where parameter β is defined by $\beta = (4/9\pi)^{1/3}$.

The effective potential for carriers is given by the sum of the initial confinement potential profile of the DFQW, Hartree term, and exchange-correlation term:

$$U_r := U_r + V_{\mathrm{Hr}} + V_{XC,r} \tag{9}$$

where the symbol := is an algorithmic equality sign for iteration purposes. To initialized, $U_r = V_{o,r}$, will be set for RHS of the expression. Inserting this new potential equation (9) into the Schrödinger equation (3) again, new energy levels and carrier distributions are obtained. By continuing this iterative looping until the values of $E_{r\ell}$ converge (within 1 meV) we obtain the self-consistent energy levels.

B. Absorption Coefficient

The absorption coefficient for the case of zero carrier injection, $\alpha_0 = \alpha\ (N = 0)$, will first be considered. The absorption coefficient with carrier injection, $\alpha_N = \alpha\ (N > 0)$, will then be determined, in which another carrier-induced effect is included: Band-filling. Band-filling accounts for a reduction in absorption for photon energies slightly above the nominal bandgap and it has been observed for several semiconductors when they are doped. This effect is most pronounced in semiconductors with small effective masses and bandgaps. In the case of n-type semiconductors, due to the sufficiently low density of states in the conduction band, only a relatively small amount of electrons can fill the band to an appreciable depth. When the lowest energy states in the conduction band are filled, electrons from the valence have to acquire energies greater than the nominal bandgap so that they can be optically excited into the conduction band. Therefore, a decrease in the absorption coefficient at energies above the bandgap is observed. The situation is similar for holes in p-type materials, but their larger effective mass means a higher density of states and hence a smaller band-filling effect for a given carrier concentration. Because band-filling is a result of free carriers, injection should be equivalent to doping, except that injection will result in band-filling effects from both the electrons and holes.

Once the electron and hole envelope wavefunctions and subband energy levels of the QW structure have been determined, the linear absorption coefficient $\alpha(\omega)$ may be determined in terms of the imaginary part of the dielectric function $\varepsilon_2(\omega)$ using the relation:

$$\alpha(\omega) = \frac{\omega\varepsilon_2(\omega)}{c_0 n_{\mathrm{Ref}}(\omega)} \tag{10}$$

where $n_{\mathrm{Ref}}(\omega)$ and c_0 are the refractive index of the DFQW [16] and the speed of light, respectively. The incoming electromagnetic radiation is taken to be propagating parallel to the xy plane (perpendicular to z axis) of the QW layer, therefore α and ε_2 are anisotropic [17] with polarization (TE or TM). Since we are interested in the QW quantization effect which manifests itself over a limited energy range above the bandgap, we use an $\varepsilon_2(\omega)$ calculation based on the direct interband transitions around the absorption edge in the Γ-valley with a parabolic band. Thus the absorption coefficient $\alpha(\omega)$ becomes [18]

$$\begin{aligned} \alpha(\omega) = \frac{\omega}{cn_{\mathrm{Ref}}\kappa_0}\sum_{c,v}|\langle\psi_c \mid \psi_v\rangle|^2 \frac{e^2\hbar^2}{6m_e E_{c,v}^2}\frac{E_g(E_g+\Delta_0)}{E_g+\frac{2}{3}\Delta_0} \\ \times \frac{(f_v-f_c)(\Gamma/2)}{(E_{c,v}-\hbar\omega)^2+(\Gamma/2)^2}\wp^{\mathrm{TE,TM}}. \end{aligned} \tag{11}$$

In (11), $\wp^{\mathrm{TE,TM}}$ is the polarization factor, fc, v is the Fermi distribution, $E_{c,v} = E_g + E_{c\ell} + E_{v\ell}, E_g$ is the intermixing induced bandgap at $z = 0$, c_o is the velocity of light in free space, κ_0 is the permittivity in free space, m_e is the effective electron mass, $n_{\mathrm{Ref}}(\omega)$ is the refractive index, Δ_0 is the spin-orbit splitting energy in the valence band, Γ is broadening factor, and the other standard physical constants having their usual values. All these parameters are functions of L_d when appropriate.

The polarization factor now accounts for both the TE and TM polarizations, and is given by [19]

$$\wp^{\mathrm{TE}} = \begin{cases} \frac{3}{4}(1+E_R), & \mathrm{hh} \\ \frac{5}{4}(1-\frac{3}{5})E_R, & \mathrm{lh} \end{cases} \tag{12a}$$

$$\wp^{\mathrm{TM}} = \begin{cases} \frac{3}{2}(1-E_R), & \mathrm{hh} \\ \frac{1}{2}(1+3E_R), & \mathrm{lh} \end{cases} \tag{12b}$$

where

$$E_R = \frac{E_{C\ell}+E_{V\ell'}}{E_{C\ell}+E_{V\ell'}+E}$$

for all possible l and l'.

The excitonic effects are included which is according to a previously published model [20]. The absorption spectrum has a typical intensity-dependent behavior, which can be described by model curves: [21]

$$\alpha(I) = \alpha_{\mathrm{linear}} + \frac{\alpha_{\mathrm{exciton}}}{1+I/I_s} \tag{13}$$

where α_{linear} represents an unsaturable backgroud absorption, $\alpha_{\mathrm{exciton}}$ is the excitonic contribution to the absorption coefficient with saturation intensity I_s.

C. Carrier-Induced Absorption Coefficient and Refractive Index Change

Once we calculate the absorption coefficient of the GaAs–$Al_wGa_{1-w}As$ QW with and without carrier injection, we are able to compute the change in absorption coefficient, $\Delta\alpha$, which is given by

$$\Delta\alpha = \alpha(\omega) - \alpha_0(\omega). \tag{14}$$

The change in refractive index $\Delta n_{\rm Ref}$, due to the change in absorption coefficient, can be calculated by the Kramers–Krönig transformation [22],[1] which is given by

$$\Delta n_{\rm Ref}(E) = \frac{c\hbar}{\pi} PV \int_0^\infty \frac{\Delta\alpha(E')}{(E')^2 - E^2}\, dE' \tag{15}$$

where PV stands for the principal Cauchy integral and $E = \hbar\omega$ is the photon energy, the units of α and E are $\rm cm^{-1}$ and eV, respectively. We now consider the last effect—free-carrier absorption. It accounts for the situation that a free carrier can absorb a photon and move to a higher energy state within a band. This involves the intraband absorption. For the intraband optical transition, the absorption is given by [18]

$$\alpha(\omega) = \frac{\omega}{cn_{\rm Ref}\kappa_0} \sum_{\ell,\ell'} \frac{|e\mu_{\ell\ell'}|(\Gamma/2)}{(E_\ell - E_{\ell'} - \hbar\omega)^2 + (\Gamma/2)^2}(N_{\ell'} - N_\ell) \tag{16}$$

where $|e\mu_{\ell\ell'}| = |\langle\psi_{r\ell}|ez|\psi_{r\ell'}\rangle|$ is the overlap integral between the ℓth and ℓ'th subbands.

On the whole, the three carrier effects: band-filling, bandgap shrinkage, and free-carrier absorption, can produce substantial contributions to the total $\Delta n_{\rm Ref}$. The band-filling and free-carrier absorption effects both produce a negative $\Delta n_{\rm Ref}$ for wavelengths in the transparent regime of the semiconductors while bandgap shrinkage produces a positive $\Delta n_{\rm Ref}$ in the same regime.

III. Results and Discussions

In this paper, we have considered the carrier-induced effects in the change of absorption coefficient as well as refractive index of GaAs–$Al_wGa_{1-w}As$ QW's in room temperature (300 K). Since the equations used depend on a number of material parameters, their value at the correct temperature is important to the accurate determination of the QW properties and hence they are listed in Table I.

The QW's to be considered here consist of the well width of 7 nm, the diffusion length is taken as 0, 1, 2, 3 nm, the Aluminum concentration is chosen as 0.2, and finally, the electron and hole concentrations are taken as $N = P = 10^{16}$, 10^{17}, 10^{18} $\rm cm^{-3}$. In addition, the conduction band offset ratio is 0.6. The full-width at half-maximum (FWHM) bound state broadening is taken as 10 meV. The broadening ratio of heavy to light hole is 1.5. In the following discussions, a default QW structure ($L_z = 7$ nm, $w_0 = 0.2$) will be used to illustrate and facilitate discussions. Other structures are similar in trend and will not be discussed explicitly here unless otherwise mentioned.

[1]For a good discussion of the Kramers–Kroenig relation, see [22].

TABLE I
List of Parameters Used in the Model

parameter	formula	Unit
E_g	1.424 + 1.594w + w(1−w)(0.127−1.31w)	eV
$m_{//e}(w)$, $m_{\perp}(w)$	$0.0632 + 0.0856w + 0.0231w^2$	m_0
$m_{\perp hh}(w)$	0.33 + 0.18w	m_0
$m_{\perp lh}(w)$	$0.088 + 0.0372w + 0.0163w^2$	m_0
$m_{//hh}(w)$	$(10.06\text{-}5.24w)^{-1}$	m_0
$m_{//lh}(w)$	$(5.24\text{-}1.98w)^{-1}$	m_0
m_0	9.109×10^{-31}	kg
κ	13.8 – 3.12	κ_0
κ_0	8.8542×10^{-12}	$\rm C(Vm)^{-1}$
n_r	see ref. 16	—
T	300	K
Q_C	0.6	—

A. DFQW Band Structure

In the model that we use, we assume that the energy at 0 eV, for the confinement profile of electrons (heavy and light holes), is taken at the bottom (top) of the conduction (valence) band without any injected carriers. We note that as L_d increases, the depth of the well decreases accordingly. However, when the carrier concentration increase, the well depth increases, which is due to the bandgap shrinkage effect. By comparing the QW bandgap transition energies, i.e., $E(e1-{\rm hh}1)$ and $E(e1-{\rm lh}1)$, for different values of L_d, and carrier concentrations. The bandgap modifications caused by changes in carrier concentration are also much smaller than those caused by changes in L_d.

When L_z is equal to 7 nm, where the Al concentration is set to 0.2 and $N = 10^{17}$ $\rm cm^{-3}$, $E(e1-{\rm hh}1)$ increases from 1.48 to 1.59 eV (blue shift of ∼110 meV) when the diffusion length is raised from 0 to 3 nm. If L_z is changed to 14.5 nm (not shown here), $E(e1-{\rm hh}1)$ increases from 1.44 to 1.49 eV (blue shift of ∼50 meV) when the diffusion length is raised from 0 to 3 nm. Therefore it is easily seen that the blue shift due to intermixing becomes less sensitive if well width is increased.

As discussed previously, the bandgap shrinkage effect gives rise to a downward (upward) shift of the confinement profile of electrons (heavy and light holes), see in Fig. 1. On the other hand, when the diffusion length increases, the QW profiles will become less confined, which results in more eigen-states to be generated. For example, when $L_z = 7$ nm, Al concentration = 0.2, $L_d = 0$, and injected carrier concentration = 10^{18} $\rm cm^{-3}$, the number of eigen-levels of heavy holes, light holes, and electrons are equal to 5, 2, and 2, respectively. However, if the diffusion length was raised to 3 nm in the above case, the corresponding three numbers equal to 10, 5, and 5, respectively.

B. Absorption Coefficients

The TE and TM polarized absorption coefficient is shown in Fig. 2 (default set) for various carrier injection levels and

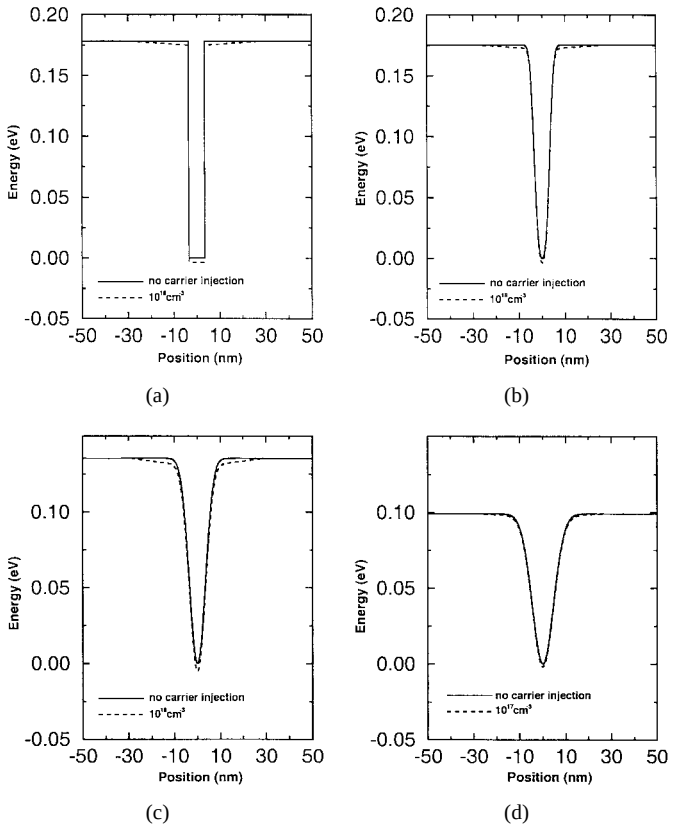

Fig. 1. Confinement profiles for electrons when $L_z = 7$ nm, Al conc. = 0.2. (a) $L_d = 0$. (b) $L_d = 1$ nm. (c) $L_d = 2$ nm. (d) $L_d = 3$ nm.

intermixing extents. A general trend to observe is that the amplitude and band-edge energy of the absorption coefficient decreases as the injected carrier concentration increases. Thus, the absorption coefficient at the edge of spectrum is at maximum (due to exciton) when no carrier injection occurs, and it continues to reduce when the injected carrier concentration increases from 10^{16} to 10^{18} (cm^{-3}) for all intermixing extents.

The carrier-induced effect, band-filling, has also been considered when calculating the absorption coefficient. This effect is taken into consideration by including a new term, $[f_v(E) - f_c(E)]$, the probability of upward transition, in our calculation of absorption coefficients. In fact, we find that this term decreases when the injected carrier concentration increases. It accounts for the major contribution of the amplitude changes for different carrier concentrations.

The absorption spectrum for TE mode is significantly different from that for TM mode, as can be seen from Fig. 2 (a)–(d) and (e)–(h), respectively. For TM mode, the saturation of lh absorption is observed for which the hh peak absorption is absent. For TE mode, both hh and lh peaks are present and the spectrum reproduces all the features observed in the usual geometry as in the unpolarized QW's. For TM mode, only the light hole peaks are observed with a slight increased of the oscillator strength. This is in good qualitative agreement with experimental results [23], [24]. According to Fig. 2(a) and (e), the first upward band-edge of the absorption spectrum of the TM mode "lags" that of the TE mode. This occurs because $E(e1 - \text{hh}1)$ is smaller than $E(e1 - \text{lh}1)$ in a lattice matched system. Also, the number of upward edges (bound state resonance) in the absorption spectrum with carrier injection ranging from 1.4 to 1.6 eV for both TE and TM modes are different. For TE mode, there are two clear upward edges while for TM mode, there is only one upward edge. The reason is that there are two possible e-hh transitions within the above range of photon energy in the former case. In the latter case, only e-lh transitions are possible, therefore only one possible e-lh transition in the above range. It accounts for the different number of upward edges in the absorption spectrum in these cases.

Another important implication that can be observed from the absorption coefficient spectrum is that the first band-edge of the absorption coefficient is blue-shifted and reduced in magnitude when the diffusion length increases, as can be observed in experiment [25]. In the above case, as shown in Fig. 2 (a)–(d), the exciton band-edge of the absorption coefficient spectrum without injected carriers occurs at around 1.475, 1.50, 1.55, and 1.59 eV when the diffusion length is taken as 0, 1, 2, 3 nm, respectively. This occurs because both $E(e1 - \text{hh}1)$ and $E(e1 - \text{lh}1)$ increases with an increasing diffusion length. As carrier concentration increases, the magnitude of absorption decreases although the band-edge energy remains about the same for most small L_d cases. This feature is observed in experiments. However as the injected carrier concentration is raised to approximately 10^{18} (cm^{-3}), the absorption edge of the QW in all four L_d cases is blue shifted to the corresponding 1.477, 1.51, 1.553, and 1.592 eV.

C. Change in Absorption Coefficient

The change in absorption coefficient ($\Delta\alpha$) is calculated by subtracting the absorption coefficient with carrier injection, α_N ($N > 0$), from that without carrier injection, α_0 ($N = 0$). From the previous section, in most cases, it is known that $\Delta\alpha$ should always be negative since α_N is always smaller than α_0 (with excitons). Moreover, because α decreases with an increasing injected carrier concentrations, we can then understand that $|\Delta\alpha|$ should be larger for the cases of higher carrier concentrations. This is also observed in experiment [17], [23].

The TE and TM polarized $\Delta\alpha$ are shown in Fig. 3(a)–(d) and (e)–(h), respectively. The $\Delta\alpha$, in general, reduces with increasing L_d because α decreases with intermixing. This effect is more enhanced for cases of high carrier injections. The shapes of the TE and TM $\Delta\alpha$ spectra are quite different. The number of downward edges for these two polarization is not equal. The reason is similar to that given in the previous section. The first downward edge of the $\Delta\alpha$ spectrum is blue-shifted when the injected carrier concentration increases. In the default set shown in Fig. 3(a)–(d) for 10^{18}-cm^{-3} carrier concentration, the peak TE absorption coefficient is about 8.5, 8, 7.5, 5.5 ($\times 1000\ \text{cm}^{-1}$) for the diffusion length $L_d = 0$, 1, 2, 3 nm respectively. If the well width is increased from 7 to 14.5 nm, not shown here, their corresponding values are 10, 8, 8, and 8 ($\times 1000\ \text{cm}^{-1}$). Also observed in the spectra is that the N-step-like feature becomes more significant in the narrow-well cases, this is because of the quantum confinement is much

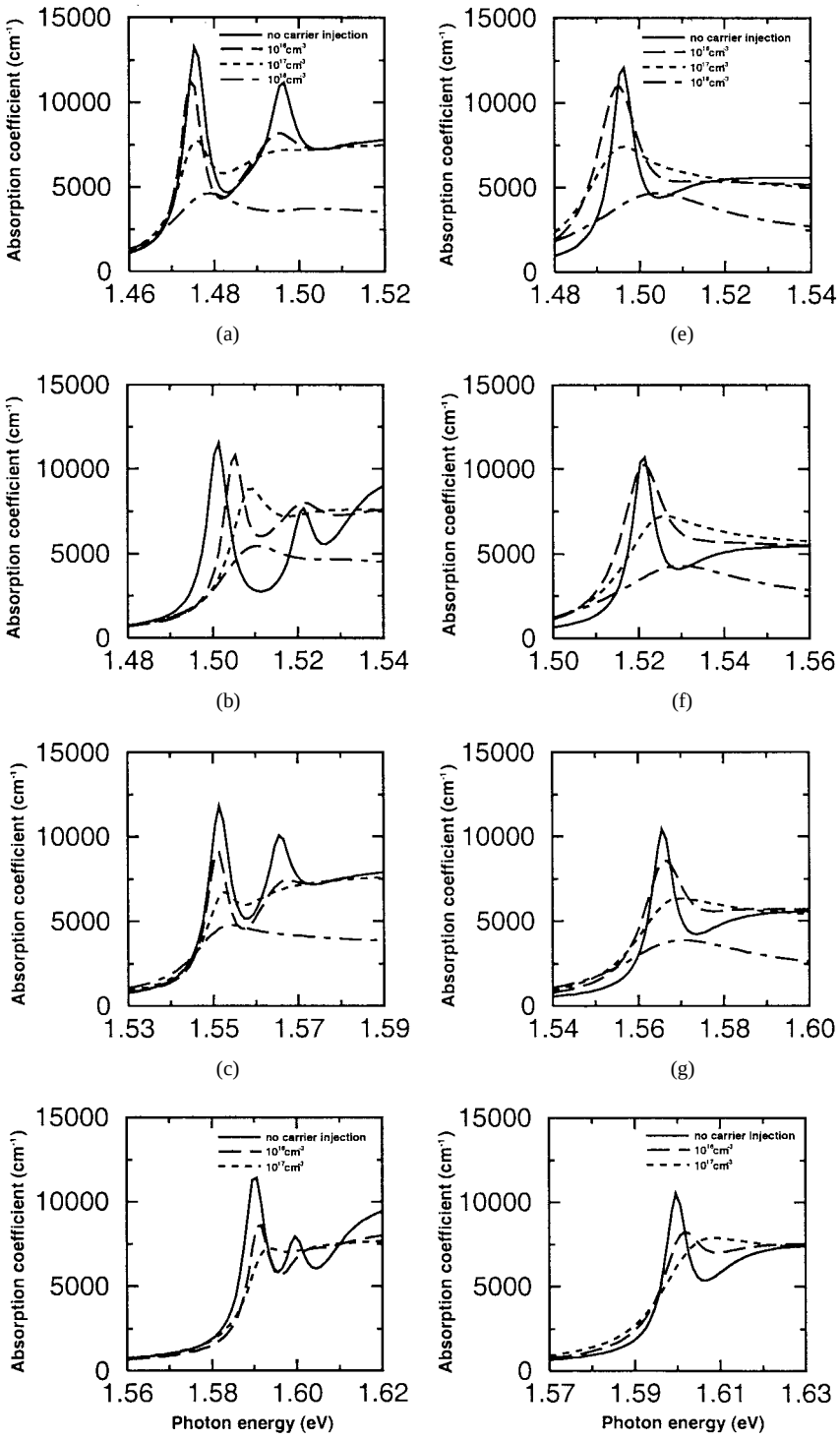

Fig. 2. Absorption coefficient α for TE mode when $L_z = 7$ nm, Al conc. $= 0.2$. TE: (a) $L_d = 0$, (b) $L_d = 1$ nm, (c) $L_d = 2$ nm, and (d) $L_d = 3$ nm. TM: (e)–(h) as in TE.

stronger here than a wider QW, which resembles a more bulk-like material in particular for large L_d. The reason is that the intermixing, if it is extensive enough, actually turns a QW material into a bulk-like averaged material. Some irregularities are shown in the spectra when carrier concentration and intermixing extent are both increased, as can be seen in Fig. 3(d) and (h).

D. Change in Refractive Index

The change in refractive index Δn_{Ref} can be obtained from $\Delta\alpha$ directly by applying the Kramers–Krönig Transformation. According to Fig. 4, it can be noted that the Δn_{Ref} spectra depend strongly on the injected carrier concentration for smaller L_d's. The amplitude of the change in refractive index increases when the injected carrier concentration increases. A

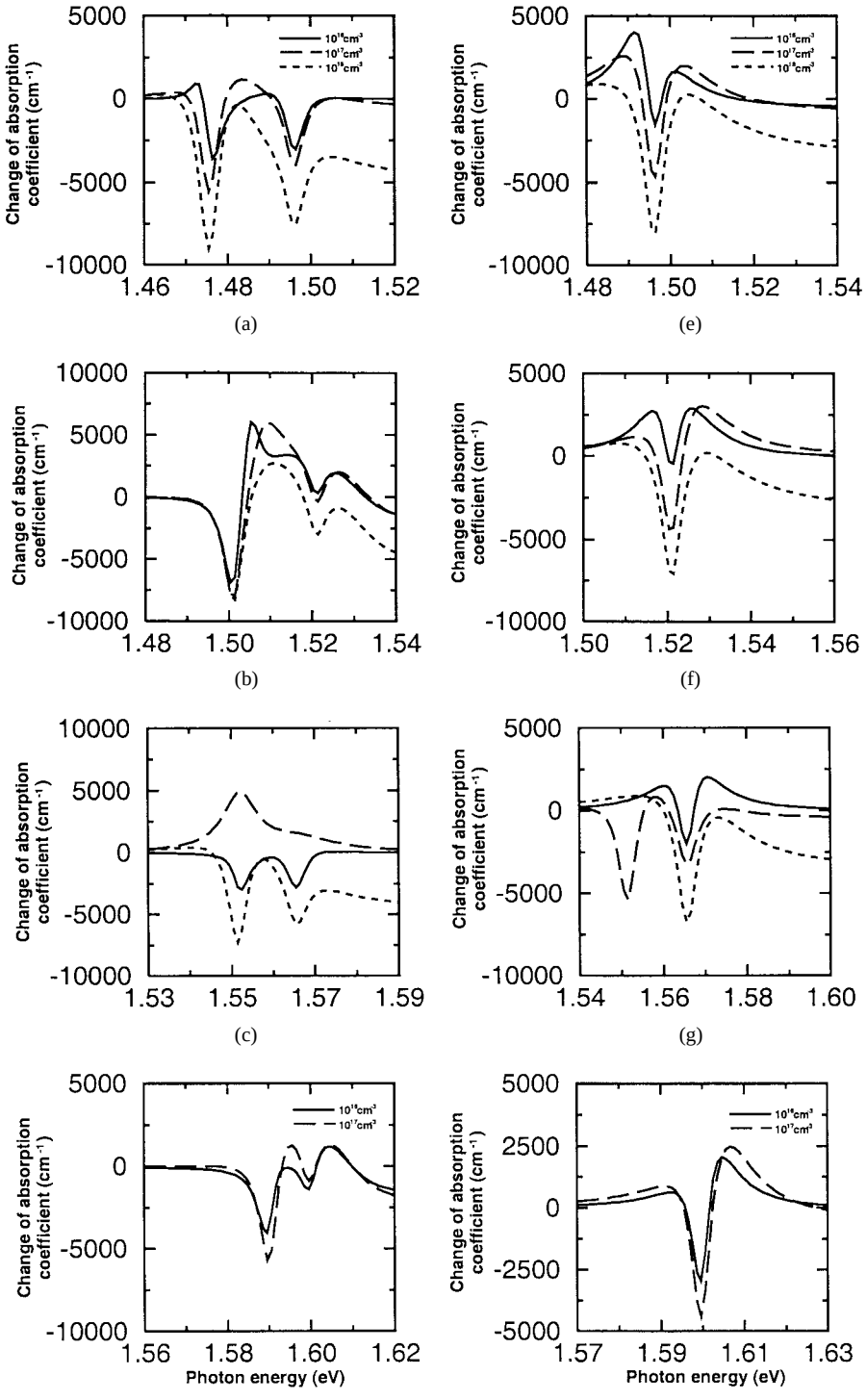

Fig. 3. Change in absorption coefficient $\Delta\alpha$ for TE mode when $L_z = 7$ nm, Al conc. = 0.2. TE: (a) $L_d = 0$, (b) $L_d = 1$ nm, (c) $L_d = 2$ nm, and (d) $L_d = 3$ nm. TM: (e)–(h) as in TE.

general trend also observed is that when the photon energy is less than the bandgap energy, the change in refractive index is very small. As the photon energy approaches the bandgap energy, the amplitude of Δn_{Ref} reaches the peak value (from negative to positive), but when the photon energy exceeds the bandgap energy, the change in refractive index again returns to a small value. This feature is observed in experimental results [26].

The position of the peak value of Δn_{Ref} is also dependent on the diffusion length L_d. It will be blue-shifted if the diffusion length increases. According to the results obtained in the previous section, for the default set with $N = 10^{18}$ cm^{-1}, Δn attains its maximum magnitude at the left N-shape dispersion when the photon energy is about 1.47–1.58 eV for the diffusion length $L_d = 0$–3 nm, see Fig. 4(a)–(d). The well width also has a significant effect

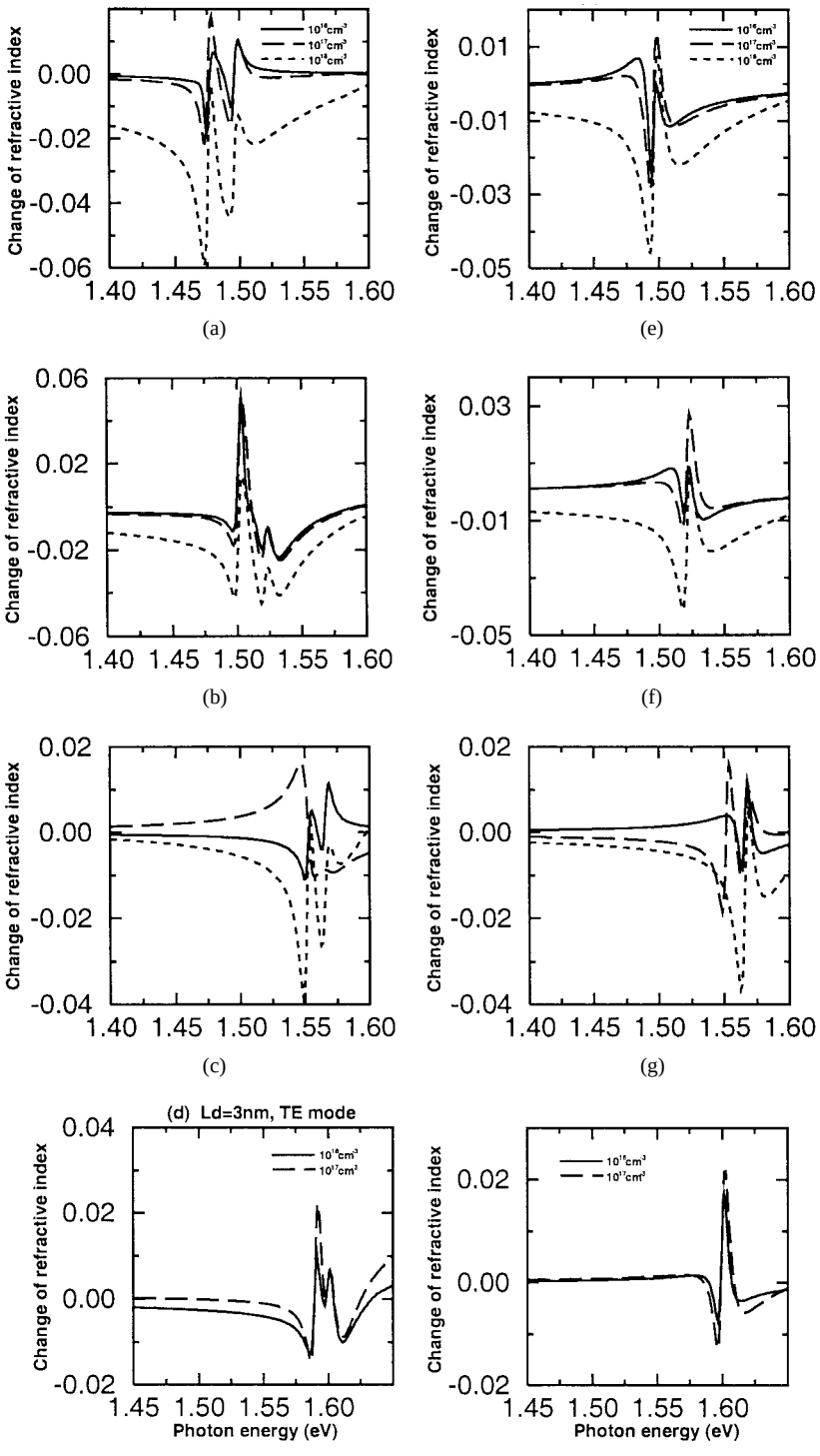

Fig. 4. Change in refractive index Δn for TE mode when $L_z = 7$ nm, Al conc. = 0.2. TE: (a) $L_d = 0$, (b) $L_d = 1$ nm, (c) $L_d = 2$ nm, and (d) $L_d = 3$ nm. TM: (e)–(h) as in TE.

on the position of the peak value of Δn. If the well width is 7 nm and Al concentration is 0.2, the peak value occurs at about 1.48 and 1.60 eV (a blue shift of 120 meV) when the diffusion length is 0 and 3 nm respectively. However, if only the well width is increased to 14.5 nm, not shown here, the peak value of Δn_{Ref} occurs at 1.52 and 1.574 eV (blue shift of only 50 meV) when the diffusion length is 0 and 3 nm respectively. Thus it implies that the blue-shift effect induced by intermixing with injected carriers is less significant in the QW structure with larger well width.

We have also considered the final carrier-induced effect in the calculation of the change of refractive index: free-carrier absorption. However, this effect is quite insignificant, as its order of magnitude is about 10^{-5}. Thus, on the whole, there are only two main carrier-induced effects that contribute to

the changes in absorption coefficient as well as in refractive index: Bandgap shrinkage, and band-filling.

IV. Conclusion

We have calculated the eigenvalues and eigenfunctions of both square QW and DFQW. The results show that as the diffusion length increases, the depth of the well decreases accordingly. However, when the carrier concentrations increase, the well depth increases due to the bandgap shrinkage. By comparing the bandgap, $E(e1-\mathrm{hh1})$, for different diffusion lengths, carrier and Al concentrations, we find that the change in diffusion length dominates the change in well depth and injected carriers. In addition, blue shift due to injected carriers is more sensitive to L_d than well width and well depth. This feature is also more enhanced for smaller L_z and large Al concentration. Moreover, when the diffusion length increases, the QW profiles will become effectively wider, which results in more eigen-pairs to be generated, and should have a larger impact to the optical properties of the QW materials.

The simplest fact observed is the amplitude of absorption coefficient decreases as the injected carrier concentration increases. The carrier-induced effect, band-filling, has also been considered when calculating absorption coefficient due to them. This effect causes a reduction in the amplitude of the absorption coefficient with the decrease in the injected carrier concentration. What is more important, the band-edge of the absorption coefficients is blue-shifted with both the diffusion length and injected carrier increases.

The sign of the change in absorption coefficient $\Delta\alpha$ is mostly negative, since the absorption coefficient with carrier injection, α_N $(N>0)$, is absolutely smaller than that without carrier injection, α_0 $(N=0)$. In addition, since α_N decreases with an increase in injected carrier concentrations, we can then understand that $|\Delta\alpha|$ should be larger for cases of higher carrier concentrations. Moreover, $\Delta\alpha$ spectrum will be blue-shifted when the diffusion length increases. Just like in the calculation of absorption coefficient, the blue-shift effect induced by different carrier concentrations would be reduced with an increase in well width. There is a jump of the magnitude of $\Delta\alpha$ between 10^{17} and 10^{18}, in other words, the optical parameters are very sensitive to the injected carrier levels above 10^{17}.

The change in refractive index Δn_{Ref} is strongly dependent on the injected carrier concentrations as well as the QW width. From the results obtained, we know that $|\Delta n|$ increases when the injected carrier concentration increases. The Δn_{Ref} is very small when the photon energy is far below the bandgap energy and reaches its peak around the bandgap energy. In addition, the position of the peak value of Δn_{rRef} is dependent on the diffusion length L_d. It will be blue-shifted if L_d increases. Moreover, the well width has a certain significance on the position of the peak value of Δn. If the well width is increased to a larger value, the blue-shift effect induced by different carrier concentrations will become less significant. Another important result worth noting, the Δn_{Ref} due to carrier is reduced for large L_d's. This should have an advantageous implication to carrier injected devices, such as lasers, since chirping can be reduced by utilizing DFQW's.

References

[1] D. Ahn and S. L. Chuang, "The theory of strained-layer quantum-well lasers with bandgap renormalization," *IEEE J. Quantum Electron.*, vol. 30, pp. 350–365, 1994.

[2] E. H. Li, Ed., *Quantum Well Intermixing for Photonics*, Milestone Series. Washington, DC: SPIE, 1998, vol. 145.

[3] J. F. Vinchant, M. Renaud, A. Goutelle, M. Erman, P. Svensson, and L. Thylén, "Low driving voltage or current digital optical switch on InP for multiwavelength system application," *Electron. Lett.*, vol. 28, pp. 1135–1137, 1992.

[4] J. F. Vinchant, J. A. Cavailles, M. Erman, P. Jarry, and M. Renauld, "InP/GaInAsP guided-wave phase modulators based on carrier-induced effects: Theory and experiments," *J. Lightwave Technol.*, vol. 10, pp. 63–70, 1992.

[5] J.-P. Weber, "Optimization of the carrier-induced effective index change in InGaAsP waveguides-application to tunable bragg filters," *IEEE J. Quantum Electron.*, vol. 30, pp. 1801–1816, 1994.

[6] C. H. Henry, R. A. Logan, and K. A. Bertness, "Spectral dependence of the change in refractive index due to carrier injection in GaAs lasers," *J. Appl. Phys.*, vol. 52, pp. 4457–4461, 1991.

[7] A. Tourita and A. Suzuki, "Carrier-induced lasing wavelength shift for quantum well laser diodes," *IEEE J. Quantum Electron.*, vol. 23, pp. 1155–1159, 1987.

[8] T. Ando and S. Mori, "Electronic properties of a semiconductor superlattices. I. Self-consistent calculation of subband structure and optical spectra," *J. Phys. Soc. Jpn.*, vol. 47, pp. 1518–1527, 1979.

[9] P. A. Chen, C. Juang, and C. Y. Chang, "Carrier-induced energy shift in GaAs/AlGaAs multiple quantum well laser diodes," *IEEE J. Quantum Electron.*, vol. 29, pp. 2607–2618, 1993.

[10] H. Yoshimura, G. E. W. Bauer, and H. Sakaki, "Carrier-induced shift and broadening of optical spectra in an $Al_xGa_{1-x}As$/GaAs quantum well with a gate electrode," *Phys. Rev.*, vol. B38, pp. 10791–10797, 1988.

[11] K. J. Kuhn, G. U. Iyengar, and S. Yee, "Free carrier induced changes in the absorption and refractive index for intersubband optical transitions in $Al_xGa_{1-x}As$/GaAs/$Al_xGa_{1-x}As$ quantum wells," *J. Appl. Phys.*, vol. 70, pp. 5010–5017, 1991.

[12] A. Kimura, M. Nido, and A. Suzuki, "Tensile-strained multiple quantum-well structures for a large refractive index change caused by current injection," *IEEE Photon. Technol. Lett.*, vol. 6, pp. 1101–1104, 1994.

[13] D. Campi, P. J. Bradley, R. Calvani, and R. Caponi, "Modeling of nonlinear absorpiton and refraction in quantum-well structures for all-optical switching," *IEEE J. Quantum Electron.*, vol. 29, pp. 1144–1157, 1993.

[14] D. J. BenDaniel and C. B. Duke, "Space-charge effects on electron tunneling," *Phys. Rev.*, vol. 152, pp. 683–692, 1966.

[15] E. H. Li, B. L. Weiss, and K. S. Chan, "Effect of interdiffusion on the subbands in an $Al_xGa_{1-x}As$/GaAs single-quantum-well structure," *Phys. Rev.*, vol. B46, pp. 15181–15192, 1992.

[16] E. H. Li, "Refractive index of Interdiffused AlGaAs/GaAs quantum wells," *J. Appl. Phys.*, vol. 82, pp. 6251–6258, 1997.

[17] J. S. Weiner, D. S. Chemla, D. A. B. Miller, H. A. Haus, A. C. Gossard, W. Wiegmann, and C. A. Burrus, "Highly anisotropic optical properties of single quantum well waveguides," *Appl. Phys. Lett.*, vol. 47, pp. 664–667, 1985.

[18] S. L. Chuang and L. Ahn, "Optical transitions in a parabolic quantum well with an applied electric field analytical solutions," *J. Appl. Phys.*, vol. 65, pp. 2822–2826, 1989.

[19] E. H. Li and B. L. Weiss, "Analytic calculation of subbands and absorption coefficients of AlGaAs/GaAs hyperbolic quantum well," *IEEE J. Quantum Electron.*, vol. 29, pp. 311–321, 1993.

[20] E. H. Li and B. L Weiss, "Exciton optical absorption in a diffusion induced nonsquare AlGaAs/GaAs quantum well," *Proc. SPIE*, 1992, vol. 1675, pp. 98–108.

[21] A. M. Fox, A. C. Maciel, M. G. Shorthose, J. F. Ryan, M. D. Scott, J. I. Davis, and J. R. Riffat, "Nonlinear excitonic absorption in GaInAs/InP quantum wells," *Appl. Phys. Lett.*, vol. 51, pp. 30–32, 1987.

[22] D. C. Hutchings, M. Sheik-Bahae, D. J. Hagan, and E. W. Van Stryland, "Kramers–Krönig relations in nonlinear optics," *Opt. Quantum Electron.*, vol. 24, pp. 1–30, 1992.

[23] J. S. Weiner, D. A. B. Miller, D. S. Chemla, T. C. Damen, C. A. Burrus, T. H. Wood, A. C. Gossard, and W. Wiegmann, "Strong polarization-sensitive electroabsorption in GaAs/AlGaAs quantum well waveguides," *Appl. Phys. Lett.*, vol. 47, pp. 1148–1150, 1985.
[24] J. D. Ralston, W. J. Schaff, D. P. Bour, and L. F. Eastman, "Room-temperature exciton electroabsorption in partially intermixed GaAs/AlGaAs quantum well wave-guides," *Appl. Phys. Lett.*, vol. 54, pp. 534–536, 1989.
[25] M. Ghisoni, P. J. Stevens, G. Parry, and J. Roberts, "Postgrowth tailoring of the optical-properties of GaAs AlGaAs quantum-well structures," *Opt. Quantum Electron.*, vol. 23, pp. S915–S924, 1991.
[26] B. R. Bennett, R. A. Soref, and J. A. Del Alamo, "Carrier-induced change in refractive index of InP, GaAs, and InGaAsP," *IEEE J. Quantum Electron.*, vol. 26, pp. 113–122, 1990.

Michael C. Y. Chan, for a biography, see this issue, p. 635.

Paul C. K. Kwok (M'78), photograph and biography not available at the time of publication.

E. Herbert Li (SM'95), for photograph and biography, see this issue, p. 582.